Available online at www.sciencedirect.com
ScienceDirect
Molecular & Biochemical Parasitology 151 (2007) 173–183
MOLECULAR & BIOCHEMICAL PARASITOLOGY

Characterisation of macrophage migration inhibitory factor from *Eimeria* species infectious to chickens☆

Katarzyna B. Miska[a,*], Raymond H. Fetterer[a], Hyun S. Lillehoj[a], Mark C. Jenkins[a], Patricia C. Allen[a], Susan B. Harper[b]

[a] *USDA/ARS, Animal Parasitic Diseases Laboratory, 10300 Baltimore Ave. BARC-East, Beltsville, MD 20705, USA*
[b] *National Institutes of Health, Office of Biotechnology Activities, 6705 Rockledge Drive, Suite 750, Bethesda, MD 20892-7985, USA*

Received 28 December 2005; received in revised form 27 October 2006; accepted 31 October 2006
Available online 27 November 2006

Abstract

Macrophage migration inhibitory factor (MIF) was the first cytokine to be identified almost 40 years ago. Homologues of MIF have been isolated recently from invertebrates, making it an interesting molecule from an evolutionary as well as functional perspective. The present study represents the first report of MIF homologues in apicomplexan parasites, belonging to the genus *Eimeria*. A single full-length clone was isolated from *Eimeria acervulina* that shared between 35 and 38% amino acid identity with MIFs of vertebrates. A MIF cDNA from *Eimeria tenella* shared 64% amino acid identity with *E. acervulina* MIF. The mRNA expression was highest in merozoites, whereas developing oocysts and sporozoites expressed low to undetectable levels. Protein expression patterns were nearly identical to that observed by reverse transcriptase polymerase chain reaction (RT-PCR), suggesting strong developmental regulation. Immunofluorescence staining and co-localisation studies of *E. acervulina* merozoites indicated that MIF is distributed throughout the cytosol, and appears to be concentrated in the apical end of the parasite. The presence of MIF was detected in excretory/secretory (ES) products collected from *E. acervulina* merozoites, and isoelectric focusing indicated that three MIF isoforms are present in this stage. Phylogenetic analysis revealed that apicomplexan MIF sequences form a sister relationship to MIF-like molecules from *Arabidopsis thaliana*.

Keywords: *Eimeria*; Macrophage migration inhibitory factor; MIF; Coccidiosis

1. Introduction

Macrophage migration inhibitory factor (MIF) was one of the first cytokines described. It was identified as a soluble protein secreted from sensitised peritoneal lymphocytes, which inhibited the migration of macrophages [1]. MIF is essential in adaptive immune responses as well as innate immunity. Mammalian MIF is an immunoregulatory molecule that affects macrophage function [2,3] resulting in inflammatory responses, inducible by pro-inflammatory molecules such as bacterial lipopolysaccharide (LPS) [4]. Because of its role in inflammation and subsequent conditions such as sepsis, shock and arthritis, the possibility of MIF as a therapeutic target is being explored [5]. The effect of MIF on adaptive immune responses is clear, since MIF antagonism suppresses T-cell activation [6] as well as delayed type hypersensitivity (DTH) responses [7]. Since its discovery, many additional functions have been ascribed to this molecule that distinguish it from other cytokines. MIF has been found to be a regulator of endocrine function [2,8], and its expression has been observed in many different cell types, including brain [9] and the β islet cells of the pancreas [10]. One of MIF's unusual features is the possession of an enzymatic thiol-protein oxidoreductase activity [11], and a tautomerase/isomerase activity [12]. The secretion of MIF also appears to be regulated by an unconventional leaderless pathway [4,13] and no MIF surface receptor has yet been found.

Abbreviations: MIF, macrophage migration inhibitory factor; ES products, excretory/secretory products; DDT, D-dopachrome tautomerase; CHMI, 5-carboxymethyl-2-hydroxymuconate isomerase; MP, maximum parsimony; NJ, neighbor joining; RT-PCR, reverse transcriptase polymerase chain reaction; LPS, lipopolysaccharide

☆ *Note:* Nucleotide sequences reported in this paper have been submitted to GenBank™, EMBL and DDBJ Databases with the accession number(s) DQ323515 and DQ323516.

* Corresponding author. Tel.: +1 301 504 5596; fax: +1 301 504 6273.
E-mail address: kmiska@anri.barc.usdau.gov (K.B. Miska).

0166-6851/$ – see front matter © 2006 Published by Elsevier B.V.
doi:10.1016/j.molbiopara.2006.10.020

In recent years, MIF orthologues have been isolated from non-vertebrate organisms, such as nematodes, *Caenorhabditis elegans* [14], *Brugia* spp. [15,16], *Trichinella* spp., *Trichuris* spp. [17,18], *Wuchereria bancrofti* and *Onchocerca volvulus* [15]. In these organisms MIF appears to have tautomerase activity as well as the ability to chemotactically induce macrophage migration [16–18]. It is unknown why a pro-inflammatory cytokine is actively expressed by parasitic nematodes, since this would not seem to be advantageous to parasites that induce a counter-inflammatory phenotype in the host [19,20]. However, there is some evidence that high MIF expression can produce anti-inflammatory effects [21,22], hypothetically resulting in MIF-mediated inflammatory suppression and subsequent immune evasion. In the free-living nematode *C. elegans*, MIF appears to be involved in homeostatic mechanisms during times of adverse conditions and stress [14]. Thus, MIF likely has multiple functions in invertebrates as well as vertebrates. An evolutionary analysis of MIF indicated that sequences from nematodes form a sister relationship to vertebrate MIFs or a sister relationship to mammalian D-dopachrome tautomerase (DDT) (an enzyme which is considered to be part of the MIF family based on sequence identity and conservation of enzymatic activity), suggesting that MIF and DDT diverged from a single ancestral gene prior to the separation of nematodes from other metazoans [23].

The present research describes the isolation and characterisation of MIF from single celled protozoans belonging to phylum Apicomplexa. Members of this phylum are all parasitic protozoa that are important in human as well as veterinary health. This study was carried out in coccidia that infect chickens, belonging to the genus *Eimeria*. These parasites are endemic and cause losses of over US$ 800 million to the poultry industry, in the US alone [24]. Characterising MIF in these protozoa allows us to begin the investigation of the biological and immunomodulatory roles that these parasites exert on the host, as well as permitting a more complete analysis of MIF evolution.

2. Materials and methods

2.1. Animals, parasites and experimental infections

Fertilised eggs of TK chickens were obtained from Hyline International Production Center (Dallas Center, IA, USA) and hatched at Animal Parasitic Diseases Laboratorie's Facilities, Agricultural Research Service, US Department of Agriculture (Beltsville, MD, USA). Chickens were kept in brooders until 3 weeks of age, at which time they were transferred to wire colony cages in separate housing for parasite infection. Chickens were inoculated per os with 2×10^6 sporulated oocysts of *Eimeria acervulina*. Preparation of oocysts used in inoculation was carried out using standard techniques described previously [25]. *E. acervulina* merozoites were harvested from the duodenal loop of chickens 89 h post-infection (p.i.) and purified using standard methods [26,27] before being pelleted and frozen at −70 °C. Purified *E. acervulina* oocysts, sporozoites and merozoites for use in mRNA expression were obtained using previously described techniques [28,29]. For immunolocalisation, *E. acervulina* merozoites were isolated from infected chickens, purified by passage over a nylon wool column, and air-dried onto multi-well slides as previously described [30]. For analysis of ES products, infected duodena recovered from birds 89 h p.i. were cut into 2–3 cm pieces and incubated in Hank's balanced salt solution (HBSS) with gentle shaking for 20–30 min. The incubation media was poured through a double layer of cheese-cloth to remove tissue and debris. The remainder of the isolation and purification protocol was carried out using previously described methods [28,29].

2.2. cDNA library construction and screening

Total RNA was isolated from frozen *E. acervulina* merozoites using TRIzol (Invitrogen, Carlsbad, CA, USA) by following the manufacturer's recommended protocol. The total RNA was resuspended in 100 μl of diethylpyrocarbonate (DEPC) treated water. The integrity of the RNA was determined by electrophoresing 1.3 μg of denatured total RNA on 1% agarose gel. Approximately 1.3 μg of total RNA was used as template for cDNA synthesis. Double stranded cDNA was generated using the SuperScript Choice System for cDNA synthesis (Invitrogen) and oligo(dT) primers. The ends of the double stranded cDNA were blunted by incubating for 45 min at 37 °C with 20 U of DNA ligase and 8 U of T4 DNA polymerase (Roche, Nutley, NJ, USA). The cDNA was ligated for 1 h at room temperature into pBluescript II KS+ vector (Stratagene, LaJolla, CA, USA) using T4 DNA ligase (Roche). Vector DNA was digested with *Eco*RV (NEB, Ipswich, MA, USA) and dephosphorylated with alkaline phosphatase (NEB) prior to ligation. Ligated cDNA was transformed into TOP10 *Escherichia coli* (Invitrogen). Random clones were picked and grown in LB/ampicillin overnight and were subsequently frozen in glycerol at −70 °C in 384-well plates. Clones were picked from glycerol stocks, and grown overnight in LB/ampicillin. Plasmid DNA was isolated using Qiaprep Miniprep Kit (Qiagen, Valencia, CA, USA).

2.3. RNA isolation and cDNA synthesis for mRNA expression analysis

All parasites used in RNA isolation were snap frozen following purification, and were stored at −70 °C until use. Total RNA was isolated from *E. acervulina*: merozoites, sporozoites and sporulated as well as unsporulated oocysts. Each sample was combined with approximately 3 g of DEPC treated Pyrex beads (3 mm diameter, Corning, Corning, NY, USA) and 10 ml of TRIzol (Invitrogen). Samples were vortexed for 1 min then incubated on ice for 1 min (4×). The remainder of the total RNA isolation protocol was carried out using the manufacturer's recommended instructions. The resulting pellets containing total RNA were resuspended in DNase/RNase free water and were stored at −70 °C. All RNA samples were treated with DNase I (Invitrogen) prior to cDNA synthesis. cDNA was synthesized from 0.8 μg of total RNA using random hexamer primers with the Advantage RT for PCR Kit (Clontech, Mountain View, CA, USA).

2.4. Expression of MIF transcripts

In order to measure the level of MIF transcripts, quantitative real-time reverse transcriptase (RT)-PCR was carried out as follows. Primers were designed to amplify 345 bp of *E. acervulina* MIF using forward primer KM161 (5′-ATGCCGCTCTGCCAGATC-3′) in combination with reverse primer KM162 (5′-GGC GAAAACGCGAGACC-3′). Primers were also designed to amplify the entire *Eimeria tenella* MIF cDNA using forward primer KM138 (5′-ATGCCACTGTGCCAGATCGTGT-3′) in combination with reverse primer KM139 (5′-TTAACCAAACACGCGGGAACCA-3′). For control purposes primers (forward primer KM97 5′-CGGTGAAACTGCGAATGGCTC-3′ and reverse primer KM98 (5′-GCCTTCCTT AGATGTGGTAGCCA-3′) that amplify a 354 bp fragment of the small subunit ribosomal RNA (SSU rRNA) from members of genus *Eimeria* were used. Reactions were carried out in triplicate using the Brilliant SYBR Green Kit (Stratagene). The Mx3000p System (Stratagene) was used in generating and detecting fluorescently labeled products. The expression of each transcript was normalized to SSU rRNA expression using the Q-gene Program [31]. The thermocycling conditions were as follows: initial heat activation of polymerase, 95 °C for 7 min; denaturation, 94 °C for 30 s; annealing, 65 °C for 30 s; extension, 72 °C for 1 min; and a final extension of 5 min at 72 °C. Cycles 2–4 were repeated 32 times.

2.5. Cloning and sequencing

Reverse transcriptase polymerase chain reaction (RT-PCR) products from both *E. tenella* and *E. acervulina* were cloned into the pCR2.1 vector using the TA Cloning Kit (Invitrogen) to confirm the amplification of appropriate genes. Inserts were sequenced using vector specific primers M13 forward and M13 reverse. All sequencing reactions were performed using the Big Dye 3.2 sequencing kits (Applied Biosystems, Foster City, CA, USA) with non-isotopic dye terminators and analyzed on an automated sequencer (Applied Biosystems 3730xl DNA Sequencer). Sequences obtained were compared with those in GenBank using the BLASTN or BLASTX algorithms [32]. Chromatograms were viewed and edited using the Sequencher 4.2 Program (Gene Codes Corp., Ann Arbor, MI, USA). Nucleotide sequence data reported in this study is available in the GenBank™, EMBL and DDBJ Databases under the accession numbers DQ323515 and DQ323516.

2.6. Recombinant MIF expression

The entire coding sequence of *E. acervulina* MIF was PCR-amplified from clone L24 using primers 134A (5′-AT**GGATCC**ATGCCGCTCTGCCAGATC-3′) and 135A (5′-ATG**AGCTCGG**CGAAAACGCGAGACC-3′) thus incorporating *Bam*HI and *Sac*I restriction sites into the resulting products. Products were digested with both *Bam*HI and *Sac*I (NEB), gel-purified using Qiagen spin columns (Qiagen), ligated into *Bam*HI–*Sac*I digested pET28(a) vector (EMD Biosciences, San Diego, CA, USA) and transformed into TOP10 cells (Invitrogen). The maintenance of the correct reading frame was confirmed by sequencing positive transformants in both directions with T7 promoter (5′-TAATACGACTCACTATAGGG-3′) and T7 terminator (5′-GCTAGTTATTGCTCAGCGG-3′) primers (EMD Biosciences). Positive clones were then transformed into *E. coli* BL21 cells (EMD Biosciences). Bacteria harboring the recombinant *E. acervulina* MIF (r*Ea*-MIF) were cultured in 50 ml of LB containing 50 μg/ml kanamycin until reaching an optical density (OD_{600}) of 0.5. Expression was induced by adding isopropyl-1-thiogalactopyranoside (IPTG) (Sigma, St. Louis, MO, USA) to a final concentration of 1 mM for 4 h at 37 °C. Cells were pelleted and frozen at −70 °C then resuspended in 2.5 ml of native binding buffer (1.2 mM NaH_2PO_4, 18.9 mM $Na_2H_2PO_4$, 0.5 M NaCl, pH 7.8) containing 1 mg/ml lysozyme (Sigma) and 0.5 mM phenylmethanesulfonyl fluoride (PMSF) (Sigma). Cells were subjected to three freeze–thaw cycles between a dry ice–ethanol bath and 37 °C water bath. RNase and DNase (1 μg/ml) were added and the samples were rocked for 30 min at room temperature. Samples were then centrifuged at 7000 rpm for 20 min at 4 °C. The resulting supernatant was loaded onto a 1 ml nickel-nitrilotriacetic acid (NiNTA) column. The column was washed five times with native binding buffer, followed by five washes with native wash buffer (12.3 mM NaH_2PO_4, 7.8 mM $Na_2H_2PO_4$, 0.5 M NaCl, pH 6.3). Recombinant protein was eluted five times with 1 ml of elution buffer (20 mM NaH_2PO_4, 0.5 M NaCl, pH 4.0). Recombinant protein was electrophoresed on 15% SDS/PAGE gel and visualized by staining with Coomasie Blue (Sigma). *E. coli* BL21 cells harboring non-recombinant pET28(a) vector were used as negative controls.

2.7. Generation of polyclonal antisera

Rabbits were housed individually in standard rabbit cages and provided standard laboratory diet with drinking water ad libitum. A blood sample was obtained from two female New Zealand White rabbits (Covance, Denver, PA, USA) prior to immunisation. Purified r*Ea*-MIF (10 μg) was mixed with ImmunoMax SR (Zonagen Corp., The Woodlands, TX, USA) adjuvant to a total volume of 500 μl and injected subcutaneously at multiple sites. Boosters were administered on day 30; on day 37 and antibody titers were measured and antisera collected.

2.8. Immunolocalisation

Merozoites were applied to multi-well slides, air-dried, and blocked with 1% BSA in PBS for 30 min at room temperature in a humid chamber. The slides were then immersed briefly (5 s) in PBS, air-dried and incubated with rabbit-anti-r*Ea*-MIF diluted 1:1000 in blocking buffer for 1 h at room temperature. Pre-immunisation serum diluted at 1:1000 was used as negative control. In order to co-localize the MIF protein staining, anti-r*Ea*-MIF stained merozoites were then incubated with a cell supernatant containing monoclonal antibody 1207

(which is identical to antibody S16P3A1) [33]. ImmunoPure TRITC-conjugated goat anti-rabbit IgG (H + L) (Sigma) and FITC-anti-mouse IgG (H + L) (Sigma) was used as a secondary antibody at a dilution of 1:100, for 1 h at room temperature. Each incubation was followed by three brief washes in PBS. After staining, slides were allowed to air-dry, were overlaid with Vectastain® mounting medium (Vector Laboratories, Burlingame, CA, USA) and a coverslip, and were examined by epifluorescence microscopy at 40× magnification. The images were captured with a Nikon DXM-1200 digital camera.

2.9. Western blots

Protein samples were analyzed by one-dimensional (1D) polyacrylamide gel electrophoresis using 1 mm thick gradient mini gels (8 cm × 9 cm, 4–12% Bis–Tris) (Invitrogen) fixed and stained as previously described [25]. Proteins were transferred to PVDF membranes (Millipore Inc., Bedford, MA, USA) by electrophoresis in a blotting chamber using 25 V for 1 h. Completeness of transfer was monitored using prestained Benchmark protein standards (Invitrogen). Magic Mark-xp Western blot standards (Invitrogen) were used to calculate relative molecular weights (MW). Following transfer, membranes were incubated in SuperBlock blocking solution (Pierce) containing 0.05% Tween-20 overnight at 4 °C. Membranes were incubated with rabbit-anti-r*Ea*-MIF, 1:500 dilution in 10% blocking solution for 1 h. Membranes were washed (3× for 10 min each) with 15 ml wash buffer (PBS with 0.05% Tween-20) and incubated for 1 h at room temperature with 10 ng/ml goat anti-rabbit antibody coupled to horseradish peroxidase (HRP) (Pierce). Membranes were washed as above and exposed to Dura Extend luminol reagent (Pierce) for 5 min. Bands were visualized with a digital camera (UVP, Upland, CA, USA).

2.10. 2D electrophoresis

For two-dimensional (2D)-electrophoresis, 10 μg of soluble merozoite proteins were precipitated from solution by incubation with acetone at −20 °C overnight. Samples were centrifuged at 20,000 × *g* for 20 min at 4 °C. The acetone was discarded and samples dried. Dried samples were dissolved in a detergent solution (8 M urea, 4% CHAPS, 40 mM Tris and 0.2 ampholytes; Reagent 2) (Bio-Rad, Hercules, CA, USA) with 2 mM tributylphosphine (TBP) as a reducing agent. Samples containing about 10 μg of protein were loaded onto 7 cm plastic strips containing an immobilized pH gradient (IPG, pH 3–10, linear gradient) (Bio-Rad) by active hydration and focused at a maximum of 4000 V for a total of 10,000 V/h with a Protean II iso-electric focusing unit (Bio-Rad). Following iso-electric focusing, IPG strips were washed sequentially for 30 min each with buffer I (6 M urea, 2% SDS, 0.37 mM Tris–HCl, pH 8.8, 20% glycerol, 130 mM dithiothreitol (DTT)) and buffer II (buffer I without DTT with 135 mM iodoacetamide). Strips were placed on top of a second dimension 4–12% Bis–Tris NuPage mini-gel (Invitrogen) and run at 200 V for approximately 1 h. Proteins were transferred to PVDF membrane and Western blot was performed as described for 1D gels.

2.11. MIF excretion/secretion

Purified merozoites (1×10^9) were incubated in 3 ml HBSS for 3 h at either 4 or 41 °C. The samples were centrifuged at 10,000 × *g* for 10 min at 4 °C and the supernatants containing ES products were removed. The ES products were concentrated and dialyzed against 50 mM Tris, pH 8.0. Protein concentration was estimated from the ratio of absorbance at 280/260 nm and samples were frozen at −70 °C. Merozoites recovered following collection of ES products were suspended in 50 mM Tris, pH 8.0, and disrupted by sonication (three cycles of 10 s each) on ice. The sample was centrifuged at 20,000 × *g* for 20 min at 4 °C and the supernatants were frozen at −70 °C. Protein concentration was determined using the BCA procedure (Pierce) with bovine serum albumin as a standard. The ES products were then subjected to Western blotting with r*Ea*-MIF antisera as described above.

2.12. Sequence and evolutionary analyses

Amino acid alignments were constructed using the ClustalX software [34] with minor manual corrections. Phylogenetic trees were reconstructed from these alignments using either the neighbor joining method (NJ) [35] to obtain evolutionary distance by calculating uncorrected *p*-value, or the maximum parsimony (MP) [36] method in PAUP*4.0b10 [37] using the heuristic search algorithm. The stability of the branching order in both the NJ as well as MP analyses was confirmed by performing 1000 bootstrap replicates. The bacterial 5-carboxymethyl-2-hydroxymuconate isomerase (CHMI) sequences were used as an outgroup. Structural analyses were carried out using SignalP V3.0 (http://www.cbs.dtu.dk/services/SignalP/) [38] and the FUGUE server (http://www-cryst.bioc.cam.ac.uk/~fugue) [39]. Putative secondary structure of *Eimeria* MIF was obtained by homology modeling using the SWISS-MODEL server (http://swissmodel.expasy.org/) [40]. The three-dimensional structure of human MIF was used as template. Protein structure was viewed using Swiss-PBDViewer software (http://ca.expasy.org/spdbv/) [41].

3. Results

3.1. Characterisation of Eimeria MIF gene

Random screening of an *E. acervulina* merozoite cDNA library identified a single clone (L24) that shared high sequence similarity (*E* value of 2e−12) with MIF described from *Petromyzon marinus* (sea lamprey) [23]. Clone L24 contained an entire open reading frame (ORF) consisting of 348 nts as well as 89 bp of 5′-untranslated region (UTR) and 224 bp of a 3′-UTR. By comparing the *E. acervulina* MIF sequence against the *E. tenella* genome using BLASTN and BLASTX algorithms (http://www.sanger.ac.uk/cgi-bin/blast/submitblast/e_tenella/omni) a single MIF homologue

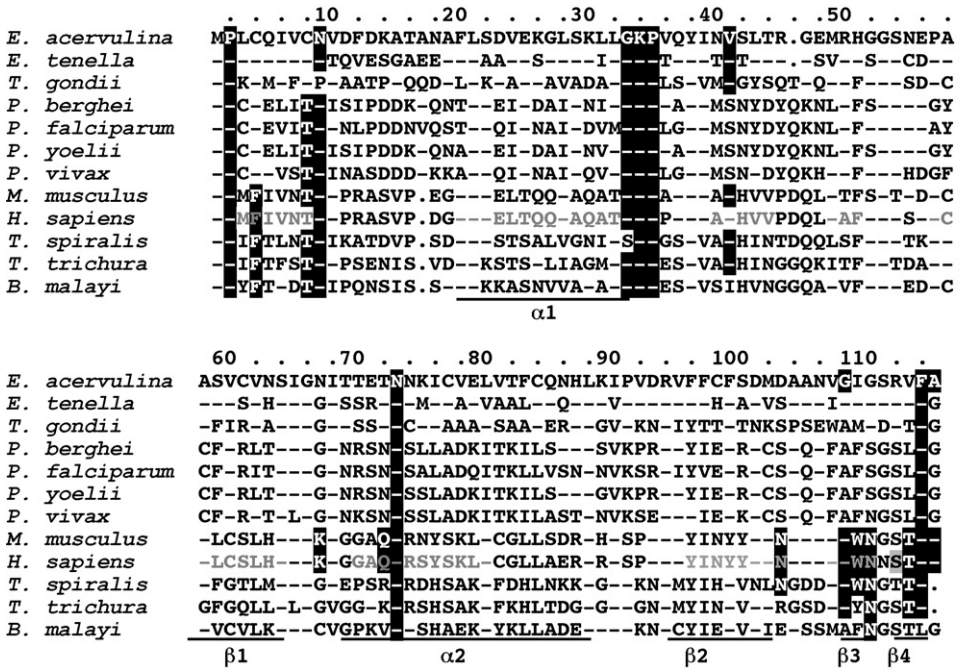

Fig. 1. Amino acid alignment of MIF proteins from different species. Regions predicted to be α-helices or β-strands in *E. acervulina* MIF are indicated at the bottom of the alignment. Regions known to be α-helical and β-strand structures in *H. sapiens* MIF are highlighted in gray. Positions believed to be involved in the formation of the catalytic site are shown on a black background. Dashes denote amino acid identity and dots denote gaps in the alignment. The amino acids are numbered according to *E. acervulina* MIF.

in the *E. tenella* genome was identified. To confirm that *E. tenella* MIF is expressed the entire ORF was amplified from cDNA of merozoites. Additional data mining uncovered MIF homologues in other apicomplexans such as *Toxoplasma gondii*, and several *Plasmodium* species. The putative apicomplexan MIFs are shown aligned in Fig. 1 with MIF molecules from two vertebrate species as well as those isolated from three species of nematodes. The MIF gene is composed of three exons and two introns and while the delineation between first and second exons is not conserved between *Eimeria* and human MIF, the boundary between second and third exons – is conserved. The amino acid identity between *E. acervulina* and *E. tenella* MIF is only 64%. There is 39% amino acid identity between *Eimeria* MIF and that of a closely related coccidian *T. gondii*, while the similarity to the sea lamprey MIF is only 1% lower. Analysis of the *Eimeria* MIF using the SignalP V3.0 software [38] indicated, that the protein lacks a signal peptide. Analysis of the protein sequence using FUGUE [39] revealed significant similarity with mammalian MIFs (*Z*-score of 29.77). Using the SWISS-MODEL server *E. acervulina* MIF was predicted to contain two α-helices and four β-sheets (underlined in Fig. 1). There are 18 amino acids that are important in the catalytic activity of vertebrate MIF [23] (shaded in black in Fig. 1) and 10 of these are identical between human and *Eimeria* MIF. The immunomodulatory activity of mammalian MIF appears to be determined by sequence of amino acids spanning from positions 50–67 in Fig. 1. In this region, mammalian MIF has been found to interact with the transcription factor JAB1 [22]. This area of MIF is also well conserved among different taxa with 53% amino acid identity between human and *Eimeria* MIF.

3.2. Developmental expression of MIF during E. acervulina life cycle

E. acervulina MIF transcripts were amplified from cDNA synthesised from oocysts collected at different time-points during sporulation, as well as sporozoites, and merozoites. The primers used in amplification were designed to span an intron, therefore PCR products generated from cDNA were smaller than those amplified from genomic DNA. MIF transcription was also determined with real-time RT-PCR using cDNA synthesized from sporulated and unsporulated oocysts, sporozoites and merozoites. The highest level of mRNA expression was observed in merozoites, while decreasing amounts of transcripts were detected in unsporulated and sporulated oocysts, respectively, with transcripts falling to undetectable levels in sporozoites (Fig. 2A). The mRNA expression profile of *E. tenella* MIF was identical to that observed in *E. acervulina* (data not shown).

Immunoblotting was carried out to analyse the level of protein expression in the same stages used above. Protein expression was similar to mRNA expression patterns with highest amounts of protein observed in merozoites, small amounts present in sporulated and unsporulated oocysts and no protein detectable in extracts from sporozoites (Fig. 2B). The polyclonal antisera generated against recombinant *E. acervulina* MIF did not cross-react against *E. tenella* MIF, therefore a protein expression profile could not be obtained. In *E. acervulina* merozoite extracts, two other bands were observed in addition to the band corresponding to MIF, at molecular weights of approximately 20 and 35 kDa. These higher molecular bands may be explained by

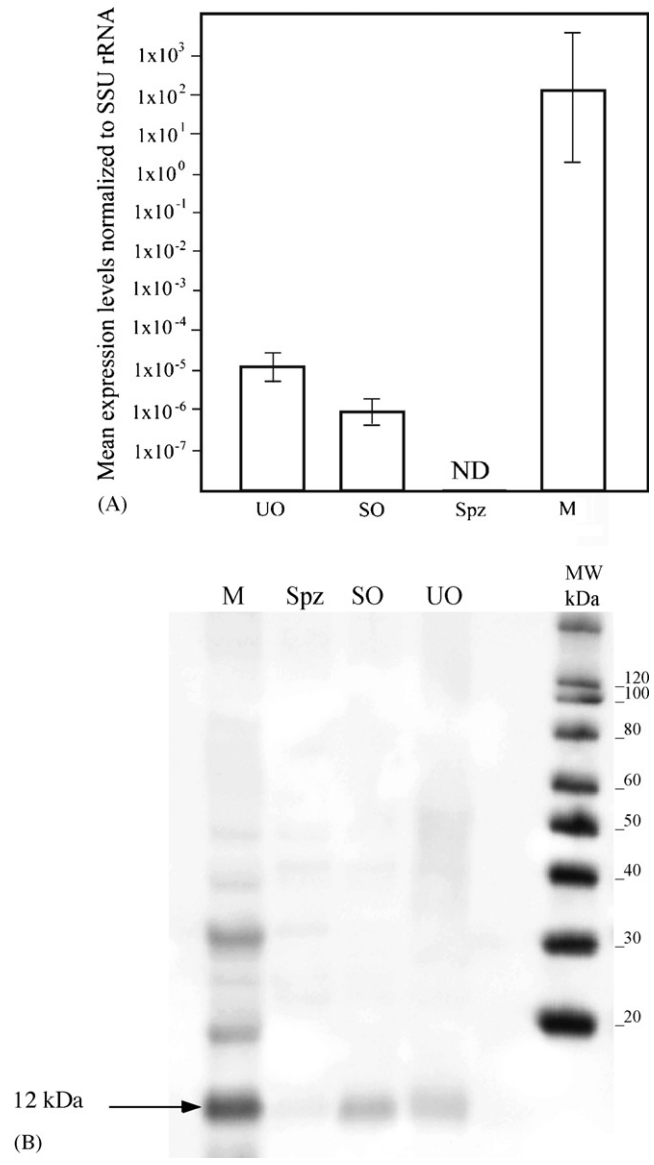

Fig. 2. (A) Analysis of expression of *E. acervulina* MIF transcripts using quantitative real-time RT-PCR showing highest levels of transcripts in merozoites. (B) Analysis of *E. acervulina* MIF protein expression using Western blotting with polyclonal antisera generated against recombinant *E. acervulina* MIF. Protein extracts from merozoites expressing highest amounts of MIF. UO, unsporulated oocysts; SO, sporulated oocysts; SPZ, sporozoites; M, merozoites; ND, no transcripts detected. Bars represent measurement of standard error.

presence of other MIF-like proteins in *E. acervulina* or presence of MIF oligomers.

3.3. Characteristics of MIF protein

An immunofluorescence assay (IFA) was performed on *E. acervulina* merozoites in order to localise MIF. Although, pre-immunisation serum shows very little reactivity (not shown), the anti-MIF antisera stained the entire parasite with greater staining intensity seen at the extreme tip of the apical end (Fig. 3A). In order to better define the localisation of MIF in the merozoites a co-localisation study was carried out using a monoclonal antibody 1207, which recognizes both surface and internal proteins of *E. acervulina* merozoites [33] (Fig. 3B). When these two images were combined it is apparent that MIF staining is cytosolic and does co-localise with the cytosolic binding pattern of antibody 1207, however, the anti-MIF antibody clearly stains the apical end of the merozoites with greater intensity.

Mammalian as well as nematode MIF is actively secreted [17] therefore ES products from *E. acervulina* merozoite were analysed for the presence of MIF. Greater amounts of MIF were observed in supernatants from merozoites incubated at 41 °C compared to 4 °C (Fig. 4). This can be compared to total extracts from merozoites that were incubated at both temperatures, in which the total amount of MIF present was comparable.

Isoelectric focusing indicated that there are three isoforms of MIF present at pH of 5.9, 6.3 and 6.7 (Fig. 5). The predicted p*I* of *E. acervulina* MIF based on the predicted amino acid sequence is 6.05. All three bands visualized by isolelectric focusing were of same molecular weight, approximately 12.0 kDa.

3.4. Evolutionary analysis of apicomplexan MIF

A protein alignment was constructed which included MIF and DDT sequences from vertebrates and invertebrates, as well as bacterial CHMI sequences which were used as an outgroup in this analysis. To reconstruct the phylogenetic relationships of the MIF family which includes the newly identified apicomplexan MIF, two methods of phylogenetic analysis were carried out, a distance method (NJ; Fig. 6) and maximum parsimony (MP). The two trees were not significantly different from each other; however, the MP tree lacked resolution in the branching pattern of distantly related sequences, and therefore is not shown. Four major groups were formed in the resulting tree (Fig. 6). The three bacterial CHMI sequences used as an outgroup formed a single group. The second group contained DDT sequences from mammals and nematodes. The third group consisted of MIF sequences from vertebrates, nematodes, and a single MIF sequence from the "Lone Star" tick, *Amblyomma americanum*. Because the tick MIF is the only MIF sequence available from any arthropod, its placement within this clade may not be reliable. The fourth group was made up of all apicomplexan MIF sequences identified thus far, which formed a sister relationship with MIF-like sequences from the plant, *Arabidopsis thaliana*. Group III that included all *bona fide* MIF sequences was sister to apicomplexan and plant MIF with 62% bootstrap support.

4. Discussion

Presence of MIF in organisms that do not possess adaptive or combinatorial immune responses raises many interesting questions regarding the function and evolution of this molecule. In the present study MIF homologues were described for the first time from single-celled parasitic protozoa belonging to phylum Apicomplexa. The full-length cDNA clone was initially discovered during a random screening of ESTs from an *E. acervulina* cDNA library. Through subsequent use of bioinformatics MIF sequences in other apicomplexans were identified, including *E. tenella*, *T. gondii* and several

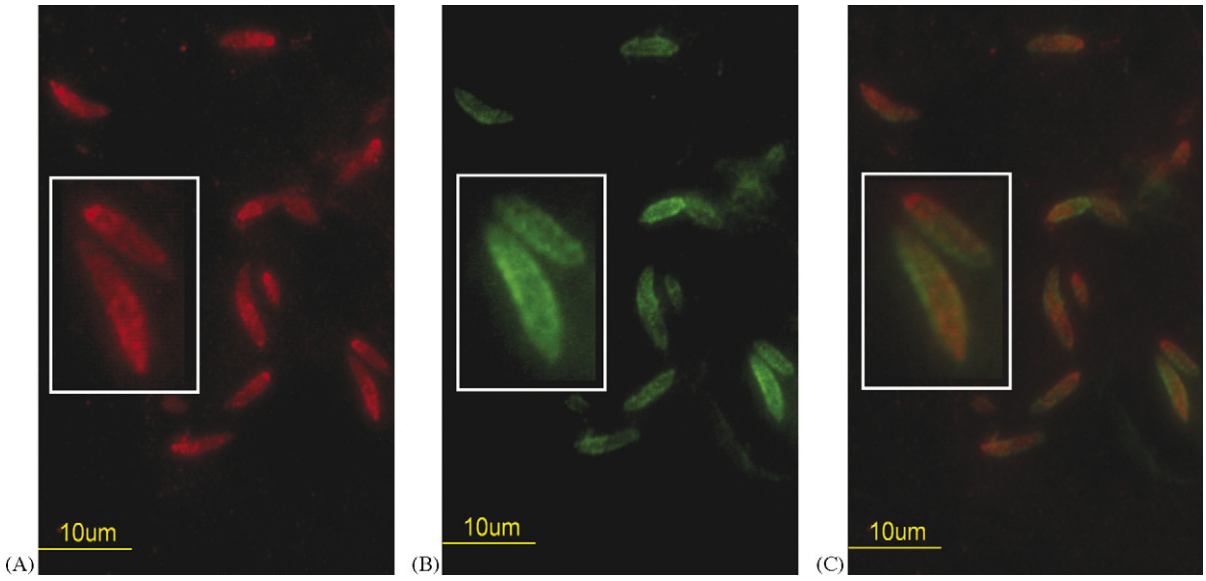

Fig. 3. Co-localisation study of MIF in *E. acervulina* merozoites. (A) *E. acervulina* merzoites stained with polyclonal antisera generated against r*Ea*-MIF, the inset shows a magnified view of two merozoites, (B) same preparation stained with monoclonal antisera 1207 recognizing surface as well as intracellular antigens and (C) a combined slide of *E. acervulina* merozoites stained with anti-r*EA*-MIF and 1207, showing cytosolic localisation of MIF with greater concentrations associated at the apical end of the merozoites.

species belonging to genus *Plasmodium*. Interestingly, MIF homologues were not found in the genomes of *C. parvum*, *C. hominis*, *Theileria parva*, *Theileria annulata*. *Babesia bovis* or *Babesia bigemina*. By identifying a single MIF-like sequence through querying the *E. tenella* genome it is likely that MIF is a single copy gene as it is also in human, mouse, cichlid, hagfish and lamprey genomes [23,42,43]. In some species, like the Chinese amphioxus multiple functional MIF copies have been found [44]. As is observed in other MIFs the *Eimeria* gene is organized into three exons and two introns [15,23,44].

Even though the primary sequence of MIF is not highly conserved between closely related species of *Eimeria* (only 64% amino acid identity observed) over half of the amino acids which

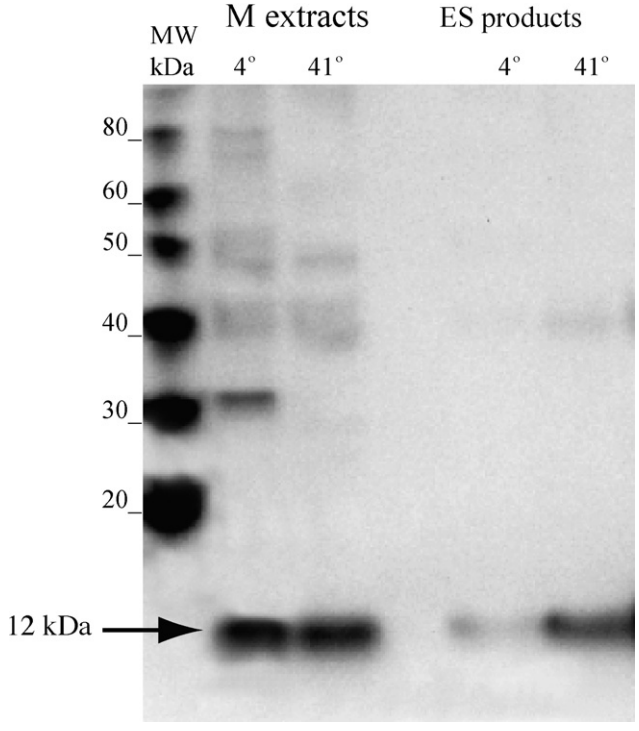

Fig. 4. Evaluation of excretory/secretory (ES) products collected from *E. acervulina* merozoites for the presence of MIF. Western blots were performed with polyclonal anti-r*Ea*-MIF antisera on soluble extracts from merozoites, or ES products from merozoites maintained at 4 or 41 °C for 3 h.

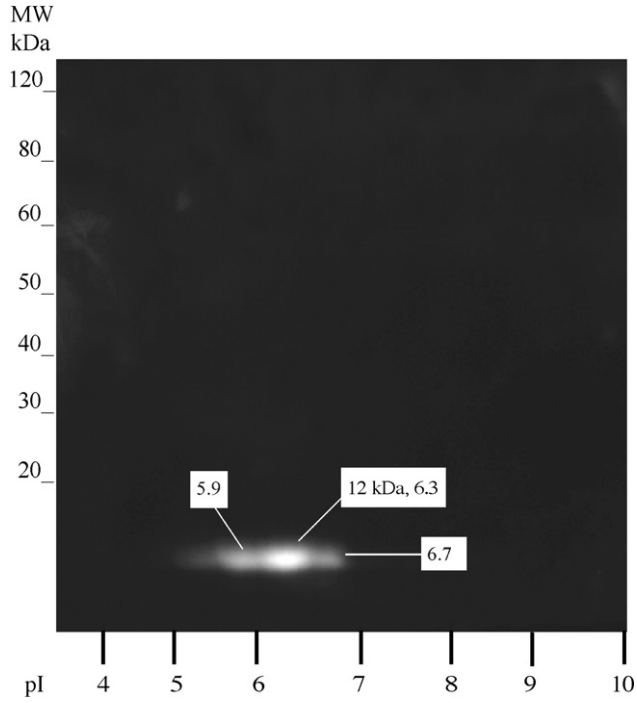

Fig. 5. Iso-electric focusing of *E. acervulina* MIF using 2D electrophoresis. Three MIF isoforms at pH 5.9, 6.3 and 6.7 were identified at MW of 12.0 kDa using polyclonal anti-r*Ea*-MIF antisera.

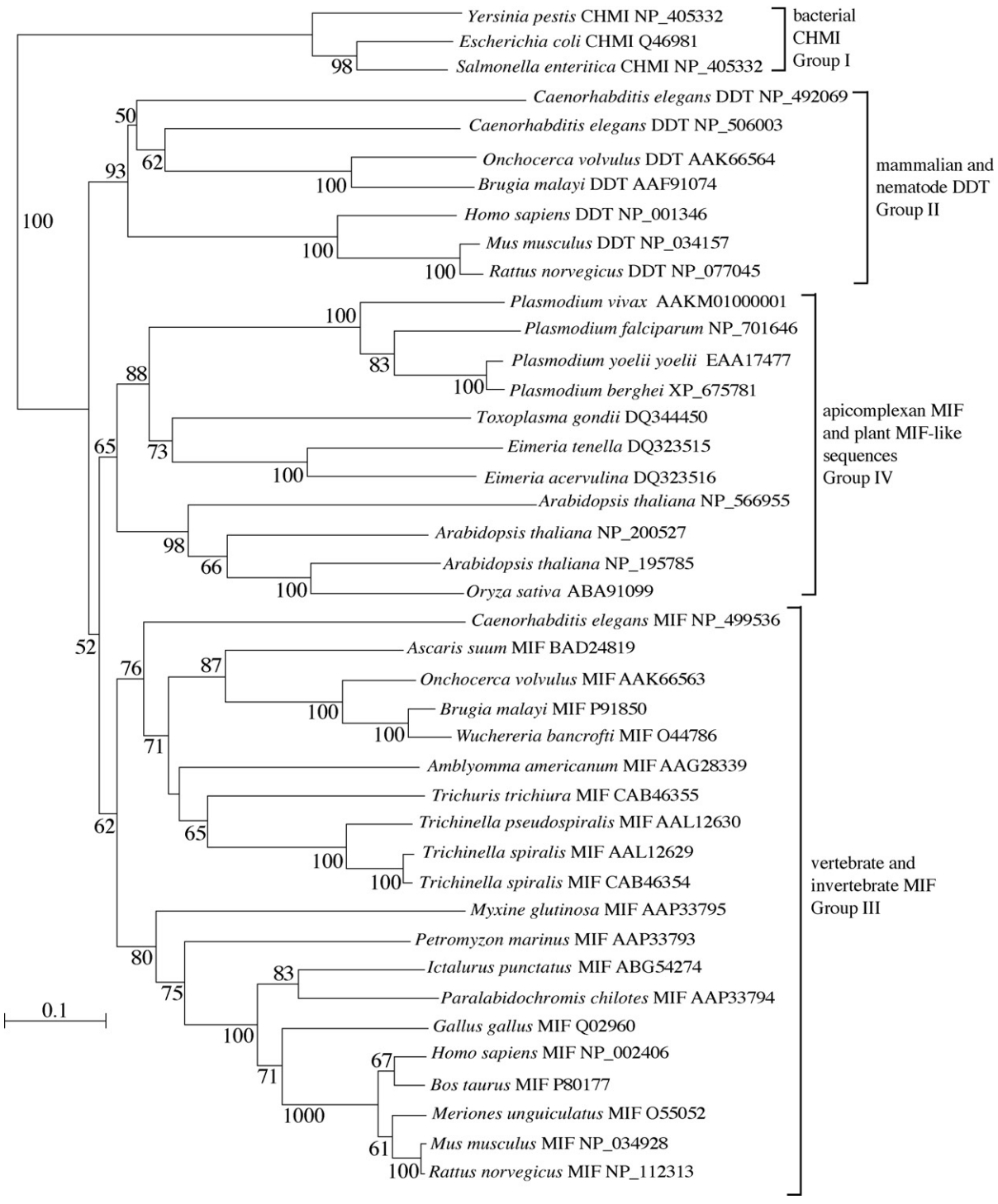

Fig. 6. Phylogenetic tree reconstructed using NJ from proteins belonging to the MIF family, including DDT, MIF and CHMI. Bacterial CHMI sequences were used as outgroup. GenBank accession numbers are shown next to the species name. Bootstrap values confirming branching order are shown next to each node. The bar indicates the measure of evolutionary distance obtained by calculating the uncorrected *p*-value. Bootstrap value of less than 50% for the branching order of *A. americanum* was not included in the figure since it is not confirmative.

form the catalytic site for enzyme activity in human and mouse MIF are identical with *Eimeria* MIF suggesting functional conservation. The three-dimensional structure of human MIF is comprised of two α-helices and six β-sheets in the following order: β1α1β2β3β4α2β5β6. The secondary structure of *Eimeria* MIF is predicted to contain two α-helices and four β-sheets, in the following order: α1β1α2β2β3β4. Therefore, the three-dimensional structures of mammalian and apicomplexan MIFs may differ, however most of the secondary structure appears to be conserved. It is worthwhile to point out that homology based modeling, which in this case employed human MIF as template may not be completely accurate, therefore only data from crystallization studies or NMR modeling will be able to provide us with the actual structure of *Eimeria* MIF.

Expression of *Eimeria* MIF transcripts as well as protein is primarily limited to the merozoite stage of the life cycle, suggesting strong developmental regulation. Merozoites represent an intracellular stage of the parasite, which are a result of rapid cell division of schizonts, and are also responsible for much of the pathology associated with coccidiosis. Comparatively, in vertebrates MIF expression is highly upregulated in response to inflammatory agents such as LPS [2,5]. In nematodes, MIF expression is present in all stages however in *Brugia malayi* it is upregulated in the adult as well as microfillariae [15]. In species of *Trichinella* as well as the free-living nematode *C. elegans* MIF is also upregulated in adult worms, while constitutively expressed in other stages [14,18]. The significance of MIF expression being primarily associated with *Eimeria* merozoites is unclear; however, it will be interesting to determine whether *Eimeria* MIF exerts effects on host responses or whether it is involved in regulatory or metabolic functions, or both. Although MIF is not detectable in *Eimeria* sporozoites, it is not known at which point after invasion of host cells by sporozoites MIF expression first becomes detectable. The kinetics of expression should be further investigated because if MIF expression is limited to merozoites, then it may be useful as a marker of merozoite presence or formation.

Eimeria MIF is present in ES products collected from merozoites. It is possible that the release of MIF could be due to active secretion or be the result of release from structurally compromised parasites. However, the amount of MIF present in ES products is a temperature sensitive process suggesting that observed secretion is a metabolically dependent process. Additionally, it has been observed that Hsp90, a protein that is not normally secreted, could not be detected in ES products of *E. acervulina* merozoites (KBM, unpublished observation). Therefore, it is likely that merozoites are remaining intact during the assay, and that secretion of MIF is a *bona fide* occurrence. In other species (vertebrates as well as invertebrates) MIF is secreted in spite of the absence of a signal peptide (a finding also observed in *Eimeria* MIF). In nematodes such as *B. malayi* [15] and in *Trichinella* spp. [17] adult worms have been shown to secrete MIF, while in vertebrate species exposure to LPS triggers MIF secretion [2,5]. The mechanism of MIF secretion in not well understood, however, it is well recognised that MIF is secreted via non-classical means [45]. Recently, the role of ABC transporters has been implicated in the mediation of MIF secretion in human monocytes [46]. Secretion of MIF may have interesting implications in apicomplexans since ABC transporters are encoded in the apicoplast genome [47] and these molecules have been implicated in drug resistance particularly in species of *Plasmodium* [48]. The immunolocalisation of *Eimeria* MIF indicates that this protein is cytosolic with greater concentration in the apical end of the merozoites. It is possible that the immunolocalisation studies reflect cross-reactivity of the polyclonal antisera with other cytosolic or apical proteins that are related to MIF, even though evolutionary analysis failed to detect MIF-related proteins in genome of *E. tenella*. It is feasible that MIF may be translated in the cytosol and targeted to the apical complex for release, however, this hypothesis is yet to be tested. Iso-electric focusing of *Eimeria* MIF indicates that three isoforms are present in merozoite extracts. Multiple isoforms have also been observed in nematodes, where two have been found in ES products of *B. malayi* [15] and three isoforms were observed in extracts of adult *Trichinella* spp. [18]. Multiple isoforms have also been observed in mammalian MIF [49], however the significance of their presence is poorly understood. Additionally, MIF is known to undergo oligomerization with dimers and trimers detected in invertebrates as well as vertebrates. The formation of these quaternary structures may affect the formation of the active site [17,50]. Oligomerization of MIF may explain presence of multiple bands that were observed in the immunoblotting analysis of *E. acervulina* merozoite extracts. Additionally MIF-related proteins of about 29.5 kDa have isolated from bovine brain extracts [51], therefore presence of such proteins could also explain higher bands observed in merozoite extracts.

It has been previously reported that MIF, DDT [52] and CHMI [53] are related or are at least similar to one another, and can be grouped into a MIF-like family. Additionally, a recent study [23] demonstrated that MIF and DDT form a sister relationship and that nematodes contain both MIF and DDT. The phylogenetic analysis reported here revealed that apicomplexan MIF sequences form a sister relationship with MIF-like sequences identified from *A. thaliana*. At this time however, none of the three plant MIF sequences have been characterized beyond their initial identification resulting from genome sequencing. It will be interesting to determine whether MIF-like proteins in plants and in apicomplexans share similar functions. As previously observed, mammalian and nematode MIF and DDT sequences formed distinct groups, with apicomplexan MIFs forming a sister relationship with *bona fide* MIF sequences. This may imply that the ancient split which gave rise to MIF and DDT genes occurred very early in eukaryotic evolution, prior to the divergence of apicomplexans. However, it must be noted, that attempts to identify DDT sequences in the genome of *E. tenella* did not produce any significant similarities. If apicomplexans lack *bona fide* DDT and but contain MIF, it is possible that MIF molecules in these species carry out functions attributed to both molecules. Because the branching order of the DDT and MIF groups cannot be ascertained since the bootstrap support for the deepest split is only 52%, it is possible that MIF and DDT diverged following the divergence of apicomplexans leading to the lack of DDT in apicomplexan genomes. Another possibility is that DDT sequences underwent a deletion in *E. tenella* and that other apicomplexans may still contain genes encoding these molecules.

In conclusion, the description of *Eimeria* MIF is the first in-depth characterisation of these molecules in protozoan organisms. This study lays the groundwork for further analysis of protozoan MIF. Characterisation of its function and the possible effects it may have on the host remain to be described.

Acknowledgements

The authors wish to thank Jenifer Herrmann, Ruth Barfield and Gary Wilkins for expert technical assistance, Matt Yamage

for construction of the *E. acervulina* cDNA library, and Dr. James Trout for critical review of the manuscript. We are also indebted to Dr. Martin Shirley for granting permission to use the *E. tenella* genome sequence available at the Sanger Institute website. This work was supported by USDA/ARS CRIS project number 1265-31320-070-00D.

References

[1] David JR. Delayed hypersensitivity in vitro: its mediation by cell-free substances formed by lymphoid cell–antigen interaction. Proc Natl Acad Sci USA 1966;56:72–7.
[2] Calandra T, Bernhagen J, Mitchell RA, Bucala R. The macrophage is an important and previously unrecognized source of macrophage migration inhibitory factor. J Exp Med 1994;179:1895–902.
[3] Onodera S, Suzuki K, Matsuno T, Kaneda K, Takagi M, Nishihira J. Macrophage migration inhibitory factor induces phagocytosis of foreign particles by macrophages in autocrine and paracrine fashion. Immunology 1997;92:131–7.
[4] Bernhagen J, Calandra T, Mitchell RA, et al. MIF is a pituitary-derived cytokine that potentiates lethal endotoxaemia. Nature 1993;365: 756–9.
[5] Morand EF. New therapeutic target in inflammatory disease: macrophage migration inhibitory factor. Int Med J 2005;35:419–26.
[6] Bacher M, Metz CN, Calandra T, et al. An essential regulatory role for macrophage migration inhibitory factor in T-cell activation. Proc Natl Acad Sci USA 1996;93:7849–54.
[7] Bernhagen J, Bacher M, Calandra T, et al. An essential role for macrophage migration inhibitory factor in the tuberculin delayed-type hypersensitivity reaction. J Exp Med 1996;183:277–82.
[8] Meinhardt A, Bacher M, McFarlane JR, et al. Macrophage migration inhibitory factor production by Leydig cells: evidence for a role in the regulation of testicular function. Endocrinology 1996;137:5090–5.
[9] Bacher M, Meinhardt A, Lan HY, et al. MIF expression in the rat brain: implications for neuronal function. Mol Med 1998;4:217–30.
[10] Waeber G, Calandra T, Roduit R, et al. Insulin secretion is regulated by the glucose-dependent production of islet beta cell macrophage migration inhibitory factor. Proc Natl Acad Sci USA 1997;94:4782–7.
[11] Kleemann R, Kapurniotu A, Frank RW, et al. Disulfide analysis reveals a role for macrophage migration inhibitory factor (MIF) as thiol-protein oxidoreductase. J Mol Biol 1998;280:85–102.
[12] Rosengren E, Bucala R, Aman P, et al. The immunoregulatory mediator macrophage migration inhibitory factor (MIF) catalyzes a tautomerization reaction. Mol Med 1996;2:143–9.
[13] Bernhagen J, Calandra T, Bucala R. Regulation of the immune response by macrophage migration inhibitory factor: biological and structural features. J Mol Med 1998;76:151–61.
[14] Marson AL, Tarr DE, Scott AL. Macrophage migration inhibitory factor (MIF) transcription is significantly elevated in *Caenorhabditis elegans* dauer larvae. Gene 2001;278:53–62.
[15] Pastrana DV, Raghavan N, FitzGerald P, et al. Filarial nematode parasites secrete a homologue of the human cytokine macrophage migration inhibitory factor. Infect Immun 1998;66:5955–63.
[16] Zang X, Taylor P, Wang JM, et al. Homologues of human macrophage migration inhibitory factor from a parasitic nematode; gene cloning, protein activity, and crystal structure. J Biol Chem 2002;277:44261–7.
[17] Tan TH, Edgerton SA, Kumari R, et al. Macrophage migration inhibitory factor of the parasitic nematode *Trichinella spiralis*. Biochem J 2001;357:373–83.
[18] Wu Z, Boonmars T, Nagano I, Nakada T, Takahashi Y. Molecular expression and characterization of a homologue of host cytokine macrophage migration inhibitory factor from *Trichinella* spp. J Parasitol 2003;89: 507–15.
[19] Maizels RM, Sartono E, Kurniawan A, Partono F, Selkirk ME, Yazdanbakhsh M. T-cell activation and the balance of antibody isotypes in human lymphatic filariasis. Parasitol Today 1995;11:50–6.
[20] Lawrence RA. Lymphatic filariasis: what mice can tell us. Parasitol Today 1996;12:267–71.
[21] Bucala R. A most interesting factor. Nature 2000;408:146–7.
[22] Kleemann R, Hausser A, Geiger G, et al. Intracellular action of the cytokine MIF to modulate AP-1 activity and the cell cycle through Jab1. Nature 2000;408:211–6.
[23] Sato A, Uinuk-ool TS, Kuroda N, et al. Macrophage migration inhibitory factor (MIF) of jawed and jawless fishes: implications for its evolutionary origin. Dev Comp Immunol 2003;27:401–12.
[24] Allen PC, Fetterer RH. Recent advances in biology and immunobiology of *Eimeria* species and in diagnosis and control of infection with these coccidian parasites of poultry. Clin Microbiol Rev 2002;15:58–65.
[25] Fetterer RH, Barfield RC. Characterization of a developmentally regulated oocyst protein from *Eimeria tenella*. J Parasitol 2003;89:553–64.
[26] Jenkins MC, Dame JB. Identification of immunodominant surface antigens of *Eimeria acervulina* sporozoites and merozoites. Mol Biochem Parasitol 1987;25:155–64.
[27] Martin A, Awadalla S, Lillehoj HS. Characterization of cell-mediated responses to *Eimeria acervulina* antigens. Avian Dis 1995;39:538–47.
[28] Miska KB, Fetterer RH, Min W, Lillehoj HS. Heat shock protein 90 genes of two species of poultry *Eimeria*: expression and evolutionary analysis. J Parasitol 2005;91:300–6.
[29] Xie MQ, Gilbert JM, Fuller AL, McDougald LR. A new method for purification of *Eimeria tenella* merozoites. Parasitol Res 1990;76:566–9.
[30] Fetterer RH, Miska KB, Jenkins MC, Barfield RC. A conserved 19-kDa *Eimeria tenella* antigen is a profilin-like protein. J Parasitol 2004;90:1321–8.
[31] Muller PY, Janovjak H, Miserez AR, Dobbie Z. Processing of gene expression data generated by quantitative real-time RT-PCR. Biotechniques 2002;32:1372–9.
[32] Altschul SF, Gish W, Miller W, Myers EW, Lipman DJ. Basic local alignment search tool. J Mol Biol 1990;215:403–10.
[33] Jenkins MC, Lillehoj HS, Danforth HD, Strohlein DA. *Eimeria acervulina*: cloning of a cDNA encoding an immunogenic region of several related merozoite surface proteins and rhoptry proteins. Exp Parasitol 1990;70:353–62.
[34] Thompson JD, Gibson TJ, Plewniak F, Jeanmougin F, Higgins DG. The ClustalX windows interface: flexible strategies for multiple sequence alignment aided by quality analysis tools. Nucleic Acids Res 1997;24:4876–82.
[35] Saitou N, Nei M. The neighbor-joining method: a new method for reconstructing phylogenetic trees. Mol Biol Evol 1987;4:406–25.
[36] Fitch WM. Toward defining the course of evolution: minimum change for a specific tree topology. Syst Zool 1971;20:406–16.
[37] Swofford DL. PAUP*: phylogenetic analysis using parsimony (* and other methods) version 4.0 beta. Sunderland, MA: Sinauer; 2002.
[38] Nielsen H, Engelbrecht J, Brunak S, von Heijne G. Identification of prokaryotic and eukaryotic signal peptides and prediction of their cleavage sites. Protein Eng 1997;10:1–6.
[39] Shi J, Blundell TL, Mizuguchi K. FUGUE: sequence–structure homology recognition using environment-specific substitution tables and structure-dependent penalties. J Mol Biol 2001;310:243–57.
[40] Schwede T, Kopp J, Guex N. Peitsch MC SWISS-MODEL: an automated protein homology-modeling server. Nucleic Acids Res 2003;31:3381–5.
[41] Guex N, Peitsch MC. SWISS-MODEL and the Swiss-PdbViewer: an environment for comparative protein modeling. Electrophoresis 1997;18:2714–23.
[42] Bozza M, Kolakowski Jr LF, Jenkins NA, et al. Structural characterization and chromosomal location of the mouse macrophage migration inhibitory factor gene and pseudogenes. Genomics 1995;27:412–9.
[43] Paralkar V, Wistow G. Cloning the human gene for macrophage migration inhibitory factor (MIF). Genomics 1994;19:48–51.
[44] Du J, Xie X, Chen H, et al. Macrophage migration inhibitory factor (MIF) in Chinese amphioxus as a molecular marker of immune evolution during the transition of invertebrate/vertebrate. Dev Comp Immunol 2004;28: 961–71.
[45] Bernhagen J, Mitchell RA, Calandra T, Voelter W, Cerami A, Bucala R. Purification, bioactivity, and secondary structure analysis of mouse

and human macrophage migration inhibitory factor (MIF). Biochemistry 1994;33:14144–55.

[46] Flieger O, Engling A, Bucala R, Lue H, Nickel W, Bernhagen J. Regulated secretion of macrophage migration inhibitory factor is mediated by a non-classical pathway involving an ABC transporter. FEBS Lett 2003;551:78–86.

[47] Cai X, Fuller AL, McDougald LR, Zhu G. Apicoplast genome of the coccidian *Eimeria tenella*. Gene 2003;321:39–46.

[48] Klokouzas A, Shahi S, Hladky SB, Barrand MA, van Veen HW. ABC transporters and drug resistance in parasitic protozoa. Int J Antimicrob Agents 2003;22:301–17.

[49] Gurvits BY, Tretyakov OY, Klishina NV, Stoeva S, Voelter W, Galoyan AA. Identification of macrophage migration inhibitory factor isoforms in bovine brain. Neurochem Res 2000;25:1125–9.

[50] Philo JS, Yang TH, LaBarre M. Re-examining the oligomerization state of macrophage migration inhibitory factor (MIF) in solution. Biophys Chem 2004;108:77–87.

[51] Cherepkova OA, Gurvits BY. Macrophage migration inhibitory factor: identification of the 30-kDa MIF-related protein in bovine brain. Neurochem Res 2004;29:1399–404.

[52] Sugimoto H, Taniguchi M, Nakagawa A, Tanaka I, Suzuki M, Nishihira J. Crystal structure of human D-dopachrome tautomerase, a homologue of macrophage migration inhibitory factor, at 1.54 Å resolution. Biochemistry 1999;38:3268–79.

[53] Subramanya HS, Roper DI, Dauter Z, et al. Enzymatic ketonization of 2-hydroxymuconate: specificity and mechanism investigated by the crystal structures of two isomerases. Biochemistry 1996;35:792–802.